Journal of
Micromechanics and
Microengineering

Integrated microfluidic systems for cell lysis, mixing/pumping and DNA amplification

INSTITUTE OF PHYSICS PUBLISHING JOURNAL OF MICROMECHANICS AND MICROENGINEERING

J. Micromech. Microeng. **15** (2005) 1215–1223 doi:10.1088/0960-1317/15/6/011

Integrated microfluidic systems for cell lysis, mixing/pumping and DNA amplification

Chia-Yen Lee[1], Gwo-Bin Lee[2,3], Jr-Lung Lin[2], Fu-Chun Huang[2] and Chia-Sheng Liao[3]

[1] Department of Mechanical and Automation Engineering, Da-Yeh University, Changhua 515, Taiwan
[2] Department of Engineering Science, National Cheng Kung University, Tainan 701, Taiwan
[3] Institute of Micro-Electro-Mechanical-System Engineering, National Cheng Kung University, Tainan 701, Taiwan

E-mail: gwobin@mail.ncku.edu.tw

Received 30 December 2004, in final form 1 March 2005
Published 29 April 2005
Online at stacks.iop.org/JMM/15/1215

Abstract

The present paper reports a fully automated microfluidic system for the DNA amplification process by integrating an electroosmotic pump, an active micromixer and an on-chip temperature control system. In this DNA amplification process, the cell lysis is initially performed in a micro cell lysis reactor. Extracted DNA samples, primers and reagents are then driven electroosmotically into a mixing region where they are mixed by the active micromixer. The homogeneous mixture is then thermally cycled in a micro-PCR (polymerase chain reaction) chamber to perform DNA amplification. Experimental results show that the proposed device can successfully automate the sample pretreatment operation for DNA amplification, thereby delivering significant time and effort savings. The new microfluidic system, which facilitates cell lysis, sample driving/mixing and DNA amplification, could provide a significant contribution to ongoing efforts to miniaturize bio-analysis systems by utilizing a simple fabrication process and cheap materials.

(Some figures in this article are in colour only in the electronic version)

Nomenclature

ASIC	application specific integrated circuit
BOE	buffered oxide etchant
C	concentration
CE	capillary electrophoresis
dNTP	deoxynucleoside triphosphates
EDL	electrical double layer
EOF	electroosmotic flow
IC	integrated circuit
LIF	laser induced fluorescence
MEMS	micro-electro-mechanical-systems
Micro-TAS	micro total analysis system
MS	mass spectrometry
PCR	polymerase chain reaction
PDMS	polydimethylsiloxane
PWM	pulse width modulator
T_{bonding}	temperature for fusion bonding process
V_{control}	control voltage to generate mixing effect ($= V_{\pm} - V_{\text{EOF}}$)
V_{EOF}	longitudinal driving potential in bulk flow
$V_{\pm}$	applied voltage to the shielding electrodes
h	the width of the microchannel
σ	mixing index

1. Introduction

MEMS technology and micromachining techniques have enabled the miniaturization of biomedical devices and systems since the 1980s. Not only do these techniques facilitate the

development of miniaturized instrumentation for biomedical analysis, but they also provide access to information at a molecular level. Micromachined biomedical systems have several advantages over their large scale counterparts, including low cost, disposability, low reagent and sample consumption, portability and lower power consumption. Significantly, the functionality and reliability of micro biomedical devices can be improved by integrating mature logic IC technology with various microfluidic devices to form a miniaturized biochip. A micro total analysis system (Micro-TAS), which integrates sample pretreatment, transportation, reaction, separation and detection on a small chip, can be realized by combining functional microfluidic components manufactured by specific MEMS technologies. Many such systems have been demonstrated in the literature, including micro-CE (capillary electrophoresis) chips [1, 2], micro-CE-MS (mass spectrometry) systems [3–5], micro-DNA chips [6–10], micro protein chips [11–17] and micro sample pretreatment systems [18].

Many approaches have been reported for the application of MEMS technologies to the fabrication of temperature control systems suitable for biomedical applications. Micro-PCR (polymerase chain reaction) chips have shown considerable potential for rapid DNA amplification. The PCR procedure is a well-developed nucleotide amplification method for genetic identification and diagnosis [19]. In theory, the concentration of a certain segment of double-stranded DNA is doubled during a thermal cycling process conducted at three different temperatures. Recently, MEMS technology has been used to miniaturize PCR systems. For example, Northrup *et al* [20, 21] presented a microfabricated, silicon-based PCR reaction chamber using boron-doped polysilicon resistors located outside of the chamber as heating elements. Fast DNA amplification has been achieved using this ingenious approach. However, the heating effect provided by these external resistors is not as efficient as when the heaters are located within the reaction chamber itself. Woolley *et al* [22] first introduced a microfabricated PCR–CE system comprising a PCR reactor integrated with capillary electrophoresis channels. The PCR reaction chamber was fabricated by bonding two Si wafers together. In their design, thermal cycling of the PCR chamber was again accomplished using polysilicon heaters, and cycling rates of 10 $^{\circ}$C s^{-1} heating and 2.5 $^{\circ}$C s^{-1} cooling were demonstrated. It was shown that their PCR–CE system was capable of DNA amplification and the separation of β-globin DNA. Alternatively, some researchers have used metal films as sensors and heaters [23, 24]. In most cases, Pt resistors were utilized both as heaters and as temperature sensors in order to simplify the design task. Most previous researchers have generally located the sensors/heaters of their micro-PCR devices outside of the PCR chamber, resulting in an imprecise temperature measurement and a low heating/cooling rate during the thermal cycle. Some previous studies used a temperature sensor located inside the PCR chamber. For example, Lagally *et al* [25, 26] developed an integrated PCR–CE system in which the Pt temperature sensors were located inside the reaction chamber while the heaters were located externally. Despite the novel design, non-uniformity of the temperature field was observed since more than 25% of volume in the chamber was 5 $^{\circ}$C less than the temperature set points. Moreover, the design was characterized by a large thermal inertia, which resulted in high power consumption and a slow frequency response. Lee *et al* presented a MEMS-based on-chip temperature control system for biomedical applications. Instead of locating temperature sensors and heating elements outside silicon chambers as reported in previous studies, high heating and cooling rate capabilities, precise temperature control and a uniform temperature field have been demonstrated since the fabricated micro temperature sensors and heaters are located within the chamber made of glass and PDMS. Besides, a glass isolation layer was utilized to avoid the interference between the metals and the DNA samples [27]. Applications of micro-PCR chips for multiple DNA amplification on five kinds of upper respiratory tract infectious diseases have also been demonstrated [28]. In general, the micro-PCR chips are more efficient, consume less sample and reagent and perform faster amplification of DNA samples.

Miniature devices for rapid sample pretreatment of DNA detection are crucial for genetic applications [29], and a rapid and efficient mixing is a necessary process in microfluidic systems designed to perform such analysis. Such devices requiring a mixing operation have traditionally relied on diffusive mixing, in which separated fluid streams are brought together within a single channel [30–35]. Three-dimensional passive and active micromixers were also reported and high mixing efficiency due to the shapes of split channels [35], rotation channels [36], impinging jets [37, 38], patterned grooves [39], fluidic networks [30] and a series of slanted wells at junctions [40], respectively, was demonstrated. However, diffusive mixing tends to be slow, and hence requires more mixing time [41]. To enhance the homogeneous mixing of samples and reagents in the PCR chamber, an active electrokinetically driven mixer utilizing zeta potential variations in the silica-based microchannels was developed [42]. Briefly, variation of zeta potential on the wall of microchannels induced by buried shielding electrodes was used for sample mixing. Efficient mixing could be achieved by applying alternating voltages on the shielding electrodes located along the microchannels. The integration of the micromixers and micro-PCR devices is of crucial importance.

In the past few years, many researchers reported various integrated microfluidic systems [43–49]. For example, Liu *et al* [43] reported an innovative $N \times N$ microfluidic matrix to perform distinct PCR reactions within 400 reactors. The integrated device was proven effective in medical diagnosis and gene testing by performing biological and chemical assays in a combinatorial manner. Lagally *et al* [44] presented an integrated portable genetic analysis microsystems including PCR amplification and capillary electrophoretic analysis coupled with a compact instrument for electrical control and laser-excited fluorescence detection. They demonstrated the feasibility of performing rapid high-quality detection of infectious diseases. Nevertheless, an efficient pretreatment system is still needed to mix samples and reagents in the integrated microsystems. Liu *et al* [45] incorporated an integrated mixer in CE chips by altering the electrophoretic mobilities of the dyes and samples. Liu *et al* [46] also developed DNA amplification and hybridization assays in integrated plastic monolithic devices utilizing syringe pumps

for reagent transport. However, the transport device was bulky and externally connected in this study. Qiao and Aluru [47] presented a compact model for electroosmotic flows in microfluidic devices, which greatly simplified the complex fluidic systems. Broyles *et al* [48] integrated sample filtration, solid-phase extraction and chromatographic separation in microfluidic devices with an on-chip transport device, which decreased size and cost of the integrated chip. The sample was electroosmotically transported through the filter element and then concentrated in the analysis channel. Recently, an integrated biochip device consisting of microfluidic mixers, valves, pumps, channels, chambers, heaters and DNA microarray sensors was developed to perform DNA analysis [49]. In spite of the full integration of DNA analysis functions in the developed biochip, the pumping and mixing devices were not on-chip devices. These external devices not only increased the size of the integrated system, but they also raised the fabrication cost.

This study presents an innovative fully automated microfluidic chip capable of performing cell lysis, electrokinetic sample/reagent transportation and mixing and DNA amplification (PCR). The various microfluidic modules are integrated on cheap and biocompatible glass substrates and on PDMS materials using a simple and reliable fabrication process. In this microfluidic device, cells are initially lyzed thermally in the micro cell lysis reactor. The DNA samples are then driven electroosmotically into a mixing section where they are mixed with PCR reagents and primers. Finally, the samples are duplicated in a micro-PCR module.

The experimental data not only confirm that the proposed microfluidic device has the ability to lyze the cells and to duplicate the DNA samples with low sample and reagent volumes, but also demonstrate that the time required to do so is significantly reduced. The developed microfluidic chip permits the transportation and mixing of samples/reagents in the connected microfluidic channels with the minimum of human intervention. Consequently, the device has considerable potential for application in generic analysis procedures.

2. Design

Figure 1 presents a schematic illustration of the proposed integrated microfluidic system, which comprises four major modules, namely a micro cell lysis reactor, a sample driving module, an electrokinetically driven micromixer and a micro-PCR chamber. A PWM (pulse width modulator) controller and an ASIC (application specific integrated circuit) are used to control the sample/reagent transport and the temperature fields inside the cell lysis reactor and the PCR chamber. As shown in figure 2, the proposed microfluidic device is in the form of a two-layered glass chip with integrated PDMS-based cell lysis and PCR chambers. Cell samples are lyzed thermally and then their DNA are extracted within the cell lysis reactor. The DNA samples are then duplicated in the micro-PCR chamber. It can be seen that the micro-heaters, micro temperature sensors and microelectrodes are deposited on the lower glass substrate. This study locates the micro sensors and micro-heaters within the PCR reaction chamber itself in order to improve the temperature measurement capabilities of the device and to

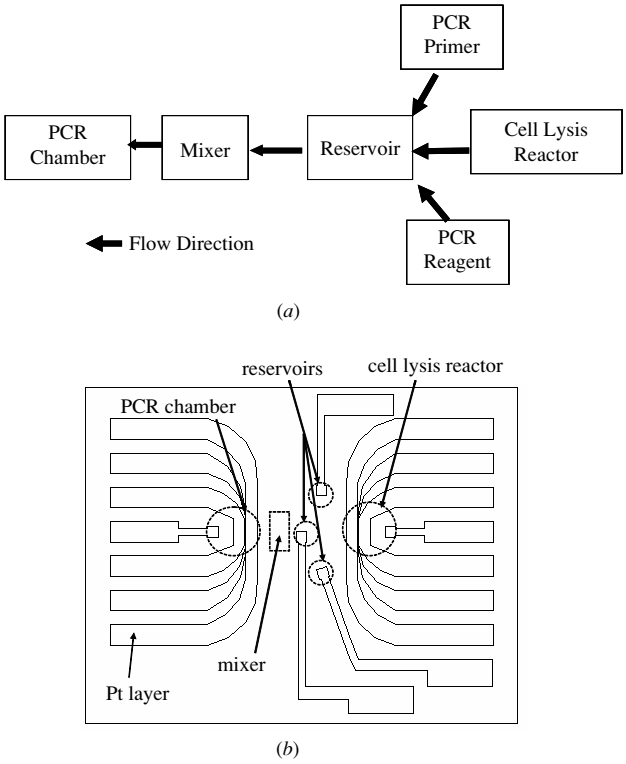

Figure 1. (*a*) Schematic representation of the integrated modules for cell lysis, mixing/pumping and DNA amplification and (*b*) top view of the lower glass substrate.

enhance its heating/cooling performance [49]. In the current design, microelectrodes are deposited on the glass substrate as the driving electrodes for EOF (electroosmosis flow) pumping [50] and on the shielding channel of the cover plate as the mixing electrodes [42].

Sample transport through the EOF channels is realized by means of electroosmotic driving forces. Note that the amount of DNA samples transported to the PCR chamber could be well controlled and has been calibrated prior to the tests of the integrated systems. Meanwhile, a mixing effect is generated through the application of an alternating electric field [42]. In this study, five pairs of buried shielding electrodes are used to shorten the fully mixing length within 4500 μm rather than using only one pair of electrodes. A glass cover plate with drilled through-holes is used to enclose the EOF channels and the mixing section. Having attached the cover plate, cover slips are adhered to the cell lysis and PCR reaction zones, respectively, to form isolation layers. Finally, PDMS chamber walls are bonded on to these isolation layers to form the cell lysis reactor and the PCR chamber, respectively. Details of the fabrication process and the characterization of the integrated chips are provided in the sections which follow [27, 42].

3. Fabrication

Figure 3 shows a simplified representation of the fabrication process adopted for the microfluidic chip. Micro-heaters and temperature sensors were formed at either end of a glass substrate to create two separate micro temperature control modules. Thin metal films were deposited on the shielding

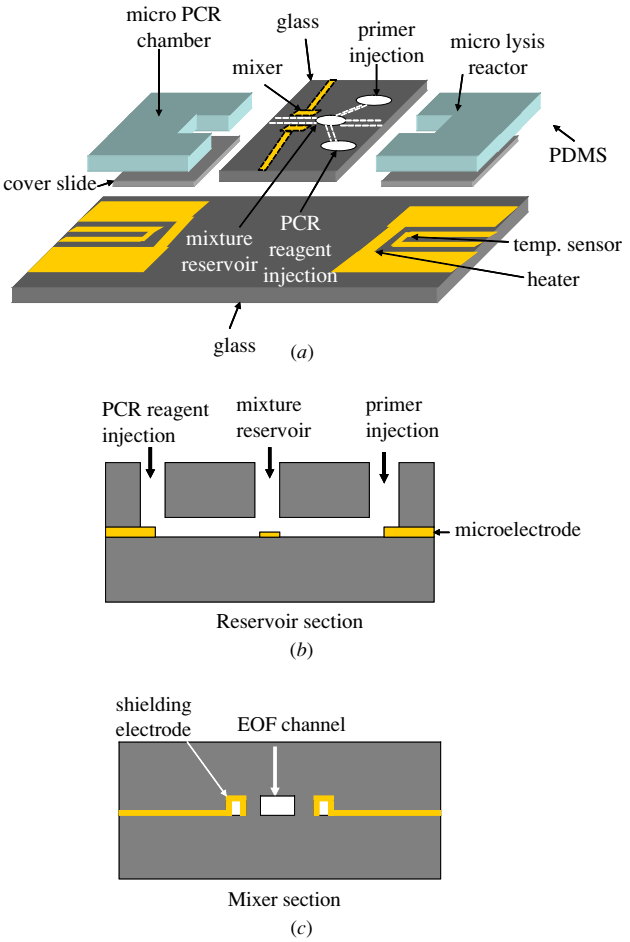

Figure 2. (*a*) Schematic representation of microfluidic chips capable of cell lysis, sample mixing and DNA amplification (PCR), (*b*) cross-section view of the reservoirs and (c) cross-section view of the mixer.

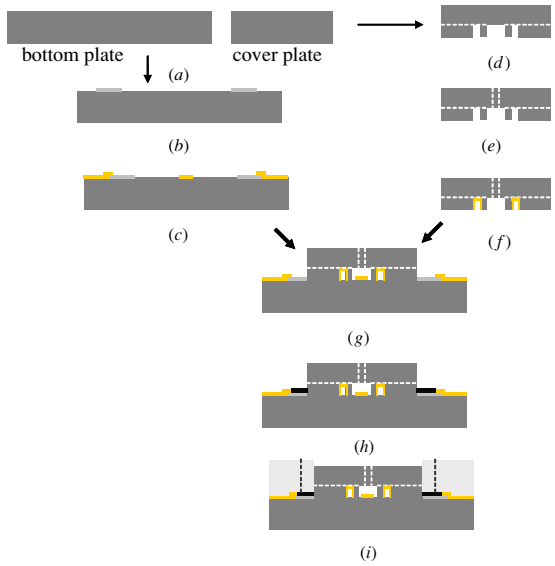

Figure 3. Simplified representation of fabrication process for microfluidic chips: (*a*) glass cleaning, (*b*) electron-beam evaporation of Pt/Cr sensors and heaters, (*c*) electron-beam evaporation of Au/Cr leads, (*d*) BOE etching of cover, (*e*) drilling, (*f*) electron-beam evaporation of Au/Cr shielding electrodes, (*g*) alignment and bonding, (*h*) attachment of cover slips and (*i*) attachment of PDMS chamber walls.

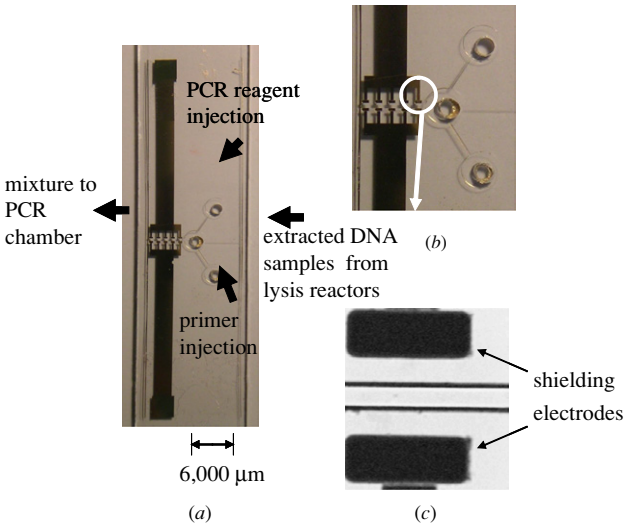

Figure 4. (*a*) Photographs of the cover plate, (*b*) mixer zone and (*c*) shielding electrodes.

channels of the cover plate to serve as shielding electrodes for mixers. Having first deposited an adhesion-enhancing thin layer of Cr (0.01 μm) on the lower glass substrate, a layer of 0.2 μm Pt was electron-beam evaporated on the Cr/glass substrate and then patterned as resistors using a standard lift-off process. It is noted that these Pt resistors served both as temperature sensors and as heaters in the integrated chip. The sensors and heaters were designed to have resistances of 100 Ω and 30 Ω, respectively. A conventional Au metallization process was used to form the necessary electrical leads (0.4 μm thickness). Meanwhile, the cover plate was etched in a 6:1 BOE bath to form microchannels of depth 25 μm. To enhance the mixing effect, a 0.4 μm thick Au layer was deposited on the shielding channels to form shielding electrodes (figure 4). Having drilled the cover plate with sample inlet holes (diameter = 2.5 mm), a fusion bonding process (T_{bonding} = 650 °C) was used to seal the microstructure and cover slips (thickness = 0.15 mm) were then attached to the lower plate to form electrical isolation layers. Au microelectrodes were also deposited on the lower glass substrate to generate the necessary driving EOF for flow transportation. However, these microelectrodes were not covered by the isolation layer of cover slips to electrokinetically drive the sample. Finally, PDMS-based chamber walls were bonded onto the cell lysis and PCR zones to form the cell lysis reactor and the PCR chamber, respectively.

4. Results and discussion

4.1. Characterization of micromixers—numerical simulation and experiment

The electroosmotic flows can be modeled by modified Navier–Stokes equations to include the body force term generated by the interaction between the excess ions of the EDL and the external electric field. The Poisson equation unifying the

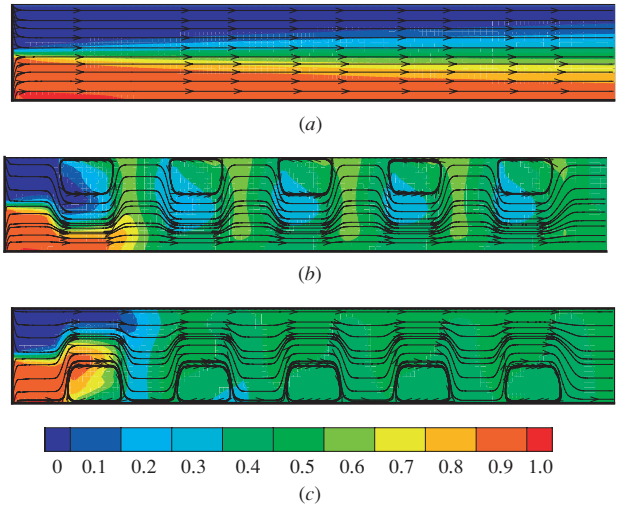

Figure 5. The streamline distributions and the corresponding concentration contour. (*a*) $t = 0$ s, (*b*) $t = 9$ s, (*c*) $t = 12$ s. The EOF driving voltage, the control voltage and the alternating frequency applied on the shielding electrodes are 20 V, 510 V and 1/6 Hz, respectively.

electric potential and zeta potential was used to compute the electric field. The ionic concentration can be computed through the Nernst–Planck equations. The simulations were performed by a commercial CFD-ACE+ software using the finite volume method. The governing equations, physical assumptions and boundary conditions were described in details, which could be found in [51].

In order to quantify the degree of mixing enhancement at any location in the microchannel, a mixing index (σ) was used which could be presented as follows [52]:

$$\sigma(x) = \left(1 - \frac{\int_o^h |C - C_\infty| \, \mathrm{d}y}{\int_o^h |C_0 - C_\infty| \, \mathrm{d}y}\right) \times 100\%, \qquad (1)$$

where C is the species concentration profile across the width of the microchannel (h), C_∞ is the completely mixed state ($= 0.5$) and C_0 is the initial unmixed state ($= 0$ or 1). Note that the confluent streams are completely mixed if $\sigma = 100\%$. In contrast, they are completely unmixed if $\sigma = 0$.

An important application of the micromixer in the microchannel is augmentation of vertical mass transfer. Figure 5 shows the numerical simulation result for a mixing region 100 μm in width and 5.5 mm in length. The EOF driving voltage, the control voltage and the alternating frequency applied on the shielding electrodes are 20 V, 510 V, and 1/6 Hz, respectively. Note that the EOF driving electrical field is only 35 V cm^{-1}, which is much less than that required to induce the sample separation in such a short channel [1, 2]. The streamline distribution and the corresponding concentration contour in the microchannel were also shown in this figure. Initially, the fluid without the activation of the micromixers lacks the transverse transportation due to the smooth streamlines (see figure 5(*a*)). Therefore, the flow shows an inefficient mixing in the microchannel. By alternating the shielding electrodes with a given frequency (1/6 Hz), the local circulation zones were formed (see figures 5(*b*) and (*c*)). The buck flow follows a significantly narrower region and more complicated route, thereby increasing the rate of diffusion by

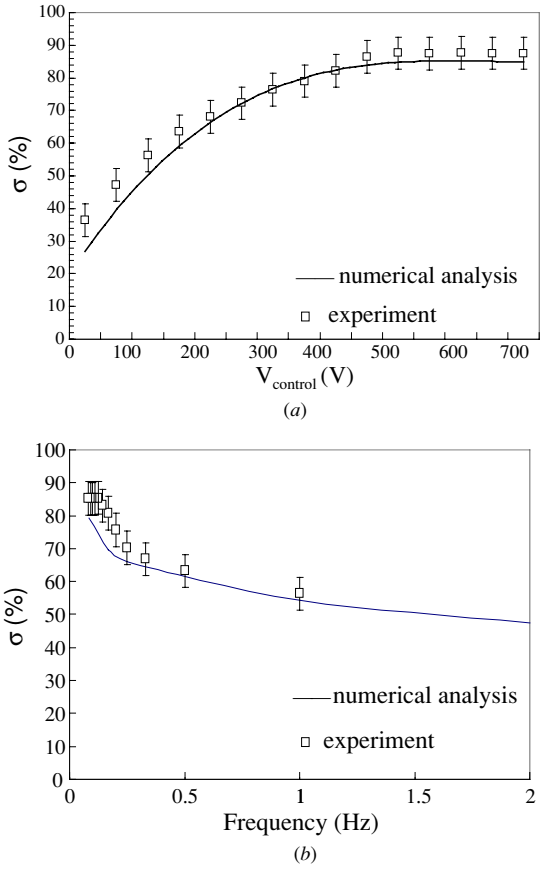

Figure 6. Experimental and simulated results for the mixing index (σ) at different control voltage (*a*) and alternating frequency (*b*). (Note: $V_{\text{control}} = V_{\pm}$ (applied voltage to the shielding electrodes) − V_{EOF} (longitudinal driving potential in EOF bulk flow).)

the local variation of zeta potential. Moreover, it is clearly seen that the flow exhibits highly efficient mixing. The mechanism of the stretching and folding will be exhibited in the fluid flow as if the shielding electrodes are driven with a given frequency.

Figure 6(*a*) indicates the relationship of the mixing index (σ) and the control voltage (V_{control}) applied to the shielding electrodes. Both numerical and experimental data were shown for comparison. Note that ten consecutive tests have been performed to get an average value of the mixing index. The variations of these experimental data are within 10%. The mixing index (σ) increases as V_{control} increases. It is clearly seen that better mixing is achieved while stronger control voltages are applied and the mixing effect is saturated when the control voltage is higher than 500 V. This phenomenon could be explained by the saturation of the zeta potential near the channel wall at high voltages [42]. Note that the driving voltage for EOF pumping is 300 V in this case. The effect of alternating frequency was also investigated. Figure 6(*b*) shows the evolution of the mixing index as a function of alternating frequency for an applied control voltage of 500 V to the shielding electrodes. Experimental and simulated data show that the mixing index (σ) decreases as driving frequency increases, indicating that a worse mixing has been achieved. Detailed information regarding the experimental set-up could be found in the previous work [42]. It indicates that effective mixing requires a certain amount of time for a slow diffusion

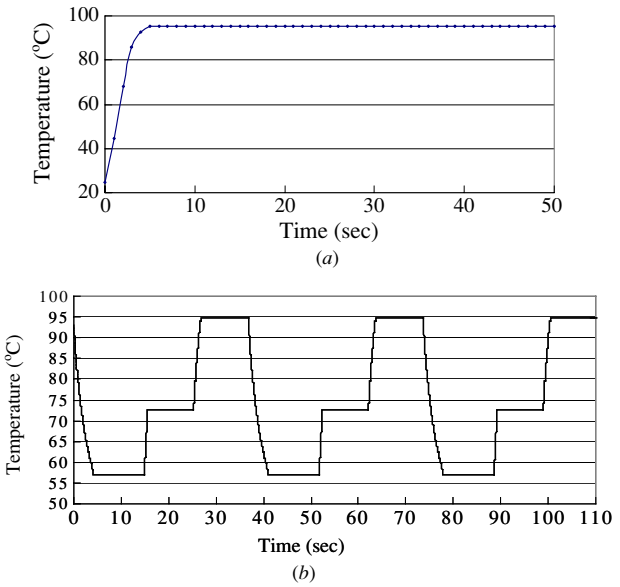

Figure 7. (*a*) Typical cell lysis temperature profile. (*b*) Typical PCR thermal cycles generated by micro temperature control system.

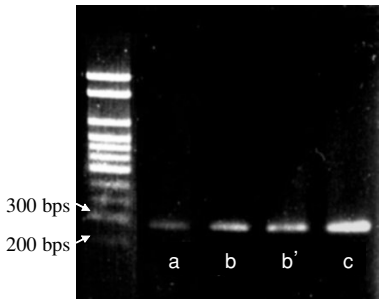

	95°C	95 °C	57 °C	72 °C	72 °C	Total time
Integrated Chip (a, b)	60sec	10sec	10sec	10sec	60sec	26 mins
Traditional PCR (c)	60sec	30sec	30sec	30sec	300sec	72 mins

30 cycles

Figure 8. Slab-gel electropherogram for pneumococcus samples (273 bps) after PCR amplification. (Note that the first lane is fluorescence signals for DNA markers. Lane a is obtained from the integrated chips without mixing and lanes b and b′ are obtained from the chips with on-chip mixing ($V_{\text{control}} = 250$ V). Lane c is obtained from a conventional PCR machine.)

process. The mixing index remains saturated for a frequency lower than 1/8 Hz. It also indicates that the active micromixer has a time constant around 4 s. Note that this time constant could vary due to dimension of the microchannels.

4.2. Characterization of DNA amplification

The micro temperature sensors enabled a real time measurement of the temperature field, while the micro-heaters provided the ability to control the temperature of the sample within the reactor/chamber precisely. The capabilities of the proposed micro cell lysis/PCR modules were investigated by considering a typical cell lysis reaction and a general PCR cycle. The results of figure 7(*a*) for a typical cell lysis reaction confirm that the integrated device is capable of maintaining the temperature at a constant 95 °C in the cell lysis reactor for 2 min of a rapid cell lysis reaction operation.

Upper respiratory tract infection microorganisms (*Streptococcus pneumoniae*) were first placed in the cell lysis reactor. After thermal lysis of the cells, the extracted DNA samples (100 ng μl^{-1}) were then driven electroosmotically by an applied EOF voltage of 20 V (V_{EOF}) to the reservoir electrodes through a microchannel full of sodium borate solution into the mixing section, where they were mixed electrokinetically by an applied external voltage of 510 V ($V_{\pm}$) to the shielding electrodes at a frequency of 1/6 Hz. An autolysin (*lyt*A) gene was used for the detection of *S. pneumoniae* [28]. PCR was performed in a total volume of 10 μl of reaction mixture containing 100 ng of template DNA, 50 pM of the 5′/3′primer, 0.1 mM dNTP (deoxynucleoside triphosphates), 1.25 mM $MgCl_2$, 1× of *Taq* buffer and 1 unit of *Taq* polymerase (Amersham; Arlington Heights, IL, USA). The resulting mixture was then driven into the PCR chamber, where PCR cycles were performed.

The amplification process involved the first DNA denaturation for 1 min at 95 °C, and a subsequent cycling involving denaturation for 10 s at 95 °C, primer annealing for 10 s at 57 °C and extension for 10 s at 72 °C with a heating rate of 20 °C s^{-1} and a cooling rate of 10 °C s^{-1}. This process was repeated for a total of 30 cycles (figure 7(*b*)). It was determined that the target DNA samples (*Streptococcus pneumoniae*) with a length of 273 bps had been amplified significantly after 30 cycles. The total time for the PCR test was 26 min 24 s and the total sample volume consumed was 15 μl. Figure 8 presents a slab-gel electropherogram of the PCR product with and without active mixing by the electrokinetically driven mixer. The fluorescence signals in the first lane represent the DNA ladders. Meanwhile, the second lane (a) shows the fluorescence signals obtained from the integrated chip without active mixing. The third lane (b) shows the fluorescence signals with active mixing using the same conditions. The DNA amplification efficiency was calculated to be 32% by a fluorescence comparison method [53]. Finally, the last lane (c) denotes the PCR products generated using a bench-top PCR machine. The experimental results demonstrate that the fluorescence signal of the actively mixed sample is stronger than that of the unmixed sample. Hence, the incorporation of an active mixer in the integrated microfluidic chip contributes significantly to the pretreatment of DNA detection. Furthermore, the developed integrated microfluidic system achieves the sample pretreatment in a shorter time and with less human intervention than conventional bench-top devices.

The dependence of the PCR products on mixing as a result of the applied control voltage ($V_{\text{control}} = V_{\pm} - V_{\text{EOF}}$) is represented experimentally in figure 9(*a*). With DNA separation and fluorescent detection in a micro-CE chip, it is clearly seen that an enhanced fluorescent intensity is induced at $V_{\text{control}} = 500$ V. As V_{control} decreases, the fluorescent intensity decreases due to the reduced DNA replication caused by inhomogeneous mixing. The intensity of the products can be calculated from the integral of the fluorescent intensity. As shown in figure 9(*b*), the intensity of the products increases as the control voltage increases due to sufficient mixing.

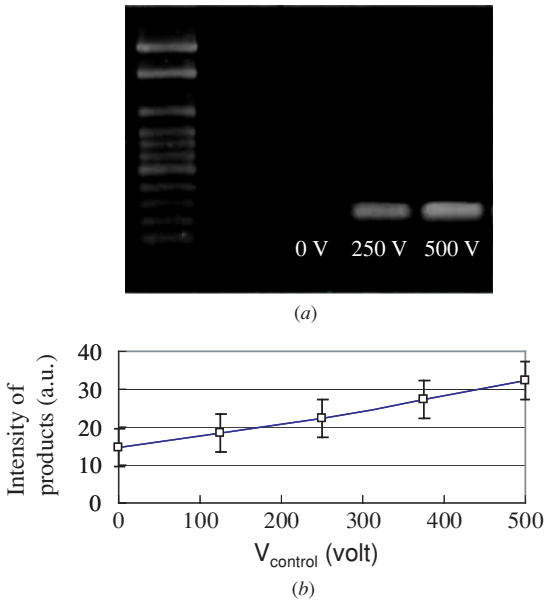

Figure 9. (*a*) Slab-gel electropherogram for *Streptococcus pneumoniae* samples (273 bps) after PCR amplification at different control voltages. (*b*) Effect of applied control voltage ($V_{control}$) on the intensity of the products. (Note that the EOF driving voltage is 20 V (45 V cm^{-1}) and the alternating frequency is 1/6 Hz.)

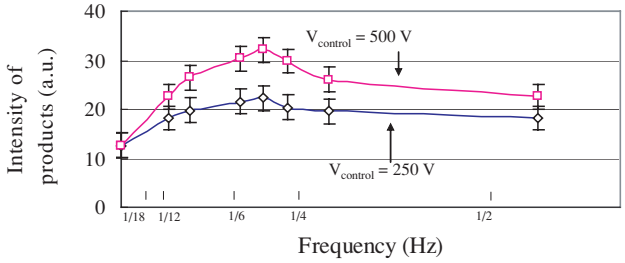

Figure 10. Effect of the alternating frequency on the intensity of the products in electropherograms for DNA samples (*Streptococcus pneumoniae)* replicated in the integrated chips at different alternating frequencies. EOF driving voltage is 20 V (45 V cm^{-1}). The total mixing time is 5 min.

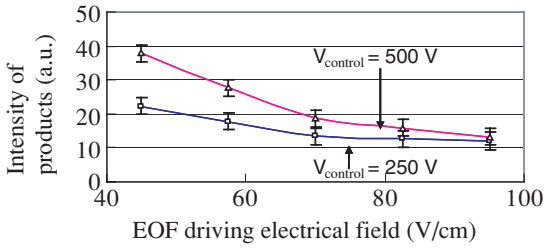

Figure 11. Effect of the EOF driving electrical field on the intensity of the products in electropherograms for DNA samples (*Streptococcus pneumoniae*) replicated in the integrated chips at different EOF driving electrical fields. Alternating frequency is 1/6 Hz. The total volume of PCR samples is 15 μl.

Figure 10 shows the evolution of the fluorescent intensity as a function of the alternating frequency for a control voltage ($V_{control} = 250$ V or 500 V) applied on the shielding electrodes. As the frequency increases from 0 Hz, the fluorescent intensity increases due to the stronger interactive mixing of the confluent streams during the traveling period. The optimal PCR result is attained at a frequency of 1/6 Hz, which therefore represents the optimal frequency of the microfluidic system. At frequencies exceeding 1/6 Hz, the fluorescent intensity decreases as driving frequency increases since the perpendicular motion of the fluid flows is insufficiently long to attain a full mixing.

The evolution of the fluorescent intensity as a function of the EOF driving electrical field is shown in figure 11. As the driving electrical field decreases, the fluorescent intensity increases due to the longer traveling time through the mixing section [42]. This observation indicates that a superior PCR result is achieved.

5. Conclusion

This study has successfully demonstrated a microfluidic system capable of performing cell lysis, sample transport, sample/reagent mixing and DNA amplification. Using MEMS techniques, this system reduces sample and reagent consumption, provides fast thermal cycling and requires minimum human intervention during its operation. Successful cell lysis and PCR amplification of a 273 bp *Streptococcus pneumoniae* have been demonstrated. It has been shown that the introduction of a device with efficient manipulation and mixing capabilities between the cell lysis reactor and the PCR chamber contributes significantly to the sample pretreatment operation in DNA detection applications. The developed integrated microfluidic system provides a powerful tool for DNA amplification, and as such represents a crucial element of the lab-on-a-chip concept.

Acknowledgments

The authors would like to thank partial financial supports from National Science Council in Taiwan (NSC 92-3112-B-006-004) and MOE Program for Promoting Academic Excellence of Universities under the grant number EX-91-E-FA09-5-4. Access of major fabrication equipment from Center for Micro/Nano Technology Research, National Cheng Kung University under projects from the Ministry of Education and the National Science Council (NSC 93-212-M-006-006) is also greatly appreciated.

References

[1] Effenhauser C S, Bruin G J M and Paulus A 1997 Integrated chip-based capillary electrophoresis *Electrophoresis* **18** 2203–13

[2] Colyer C L, Tang T, Chiem N and Harrison D J 1997 Clinical potential of microchip capillary electrophoresis systems *Electrophoresis* **18** 1733–41

[3] Xu N, Lin Y, Hofsadler S A, Matson D, Call C J and Smith R D 1998 A micro fabrication dialysis device for sample cleanup in electrospray ionization mass spectrometry *Anal. Chem.* **70** 3553–6

[4] Kane R S, Glink P T, Chapman R G, McDonald J C, Jensen P K, Gao H, Pasa-Tolic L, Smith R D and Whitesides G M 2001 Basicity of the amino groups of the aminoglycoside amikacin using capillary electrophoresis and coupled CE–MS–MS techniques *Anal. Chem.* **73** 4028–36

[5] Kameoka J, Craighead H G, Zhang H and Henion J 2001 A polymeric microfluidic chip for CE/MS determination of small molecules *Anal. Chem.* **73** 1935–41
[6] Erill I, Campoy S, Rus J, Fonseca L, Ivorra A, Navarro Z, Plaza J A, Aguiló J and Barbé J 2004 Development of a CMOS-compatible PCR chip: comparison of design and system strategies *J. Micromech. Microeng.* **14** 1558–68
[7] Ali M F, Kirby R, Goodey A P, Rodriguez M D, Ellington A D, Neikirk D P and McDevitt J T 2003 DNA hybridization and discrimination of single-nucleotide mismatches using chip-based microbead arrays *Anal. Chem.* **75** 4732–9
[8] Xu Y, Vaidya B, Patel A B, Ford S M, McCarley R L and Soper S A 2003 Solid-phase reversible immobilization in microfluidic chips for the purification of dye-labeled DNA sequencing fragments *Anal. Chem.* **75** 2975–84
[9] Kaji N, Tezuka Y, Takamura Y, Ueda M, Nishimoto T, Nakanishi H, Horiike Y and Baba Y 2004 Separation of long DNA molecules by quartz nanopillar chips under a direct current electric field *Anal. Chem.* **76** 15–22
[10] Erickson D, Liu X, Krull U and Li D 2004 Electrokinetically controlled DNA hybridization microfluidic chip enabling rapid target analysis *Anal. Chem.* **76** 7269–77
[11] Sanders G H W and Manz A 2000 Chip-based microsystems for genomic and proteomic analysis *Trends Anal. Chem.* **19** 364–78
[12] Bi L J, Zhou Y F, Zhang X E, Deng J Y, Zhang Z P, Xie B and Zhang C G 2003 A MutS-based protein chip for detection of DNA mutations *Anal. Chem.* **75** 4113–19
[13] Angenendt P, Glokler J, Konthur Z, Lehrach H and Cahill D J 2003 3D protein microarrays: performing multiplex immunoassays on a single chip *Anal. Chem.* **75** 4368–72
[14] Xiao D, Le T V and Wirth M J 2004 Surface modification of the channels of poly(dimethylsiloxane) microfluidic chips with polyacrylamide for fast electrophoresis separations of proteins *Anal. Chem.* **76** 2055–61
[15] Renzi R F, Stamps J, Horn B A, Ferko S, VanderNoot V A, West J A A, Crocker R, Wiedenman B, Yee D and Fruetel J A 2005 Hand-held microanalytical instrument for chip-based electrophoretic separations of proteins *Anal. Chem.* **77** 435–41
[16] Kojima K, Hiratsuka A, Suzuki H, Yano K, Ikebukuro K and Karube I 2003 Electrochemical protein chip with arrayed immunosensors with antibodies immobilized in a plasma-polymerized film *Anal. Chem.* **75** 1116–22
[17] Warren E N, Elms P J, Parker C E and Borchers C H 2004 Development of a protein chip: a MS-based method for quantization of protein expression and modification levels using an immunoaffinity approach *Anal. Chem.* **76** 4082–92
[18] de Mello A J and Beard N 2003 Dealing with 'real' samples: sample pre-treatment in microfluidic systems *Lab Chip* **3** 11N–19N
[19] Mullis K B, Ferré F and Gibbs R A 1994 *The Polymerase Chain Reaction* (Basle: Birkhäuser)
[20] Northrup M A, Ching M T, White R M and Watson R T 1993 DNA amplification with a microfabricated reaction chamber *Proc. Transducers* pp 924–6
[21] Northrup M A, Gonzalez C, Hadley D, Hills R F, Landre O, Lehew S, Saiki R, Shinsky J J, Watson R and Watson R Jr 1995 A MEMS-based miniature DNA analysis system *Proc. Transducers* pp 764–7
[22] Woolley A T, Hadley D, Landre P, de Mello A J, Mathies R A and Northrup M A 1996 Functional integration of PCR amplification and capillary electrophoresis in a microfabricated DNA analysis device *Anal. Chem.* **68** 4081–6
[23] Daniel J H, Iqbal S, Millington R B, Moore D F, Lowe C R, Leslie D L, Lee M A and Pearce M J 1998 Silicon microchambers for DNA amplification *Sensors Actuators* A **71** 81–8
[24] Schanmueller C G J, Lee M A, Evans A G R, Brunnschweiler A and Leslie D L 2000 Closed chamber PCR chips for DNA amplification *Eng. Sci. Educ. J.* **Dec** 259–64
[25] Lagally E T and Mathies R A 2001 Integrated PCR–CE system for DNA analysis to the single molecule limit *Proc. Micro Total Analysis Systems* pp 117–18
[26] Lagally E T, Simpson P C and Mathies R A 2000 Monolithic integrated microfluidic DNA amplification and capillary electrophoresis analysis system *Sensors Actuators* B **63** 138–46
[27] Lee C Y, Lee G B, Liu H H and Huang F C 2002 MEMS-based temperature control system for PCR applications *Int. J. Non-linear Sci. Numer. Simul.* **3** 215–18
[28] Liao C S, Lee G B, Wu J J, Chang C C, Hsieh T M and Luo C H 2005 Micromachined polymerase chain reaction system for multiple DNA amplification of upper respiratory tract infectious diseases *Biosens. Bioelectron.* **20** 1341–8
[29] Namasivayam V, Lin R, Johnson B, Brahmasandra S, Razzacki Z, Burke D T and Burns M A 2004 Advances in on-chip photodetection for applications in miniaturized genetic analysis systems *J. Micromech. Microeng.* **14** 81–90
[30] Detinger S K W, Chiu D T, Jeon N L and Whitesides G M 2001 Generation of gradients having complex shapes using microfluidic networks *Anal. Chem.* **73** 1240–6
[31] Gobby D, Angeli P and Gavriilidis A 2001 Mixing characteristics of T-type microfluidic mixers *J. Micromech. Microeng.* **11** 126–32
[32] Veenstra T T, Lammerink T S J, Elwenspoek M C and van den Berg A 1999 Characterization method for a new diffusion mixer applicable in micro flow injection analysis systems *J. Micromech. Microeng.* **9** 199–202
[33] He B, Burke B J, Zhang X, Zhang R and Regnier F E 2001 A picoliter-volume mixer for microfluidic analytical systems *Anal. Chem.* **73** 1942–7
[34] Burke B J and Regnier F E 2003 Stopped-flow enzyme assays on a chip using a microfabricated mixer *Anal. Chem.* **75** 1786–91
[35] Bessoth F G, de Mello A J and Manz A 1999 Microstructure for efficient continuous flow mixing *Anal. Commun.* **36** 213–15
[36] Park S J, Kim J K, Park J, Chung S, Chung C and Chang J K 2004 Rapid three-dimensional passive rotation micromixer using the breakup process *J. Micromech. Microeng.* **14** 6–14
[37] Yang R, Williams J D and Wang W 2004 A rapid micro-mixer/reactor based on arrays of spatially impinging micro-jets *J. Micromech. Microeng.* **14** 1345–51
[38] Koch M, Chatelain D, Evans A G R and Brunnschweiler A 1998 Two simple micromixers based on silicon *J. Micromech. Microeng.* **8** 123–6
[39] Wang H, Iovenitti P, Harvey E and Masood S 2003 Numerical investigation of mixing in microchannels with patterned grooves *J. Micromech. Microeng.* **13** 801–8
[40] Johnson T J, Ross D and Locascio L E 2002 Rapid microfluidic mixing *Anal. Chem.* **74** 45–51
[41] Nguyen N T and Wu Z 2005 Micromixers—a review *J. Micromech. Microeng.* **15** R1–16
[42] Lee C Y, Lee G B, Fu L M, Lee K H and Yang R J 2004 Electrokinetically-driven active flow controllers utilizing zeta potential variation in silica-based microchannels *J. Micromech. Microeng.* **14** 1390–8
[43] Liu J, Hansen C and Quake S R 2003 Solving the 'world-to-chip' interface problem with a microfluidic matrix *Anal. Chem.* **75** 4718–23
[44] Lagally E T, Scherer J R, Blazej R G, Toriello N M, Diep B A, Ramchandani M, Sensabaugh G F, Riley L W and Mathies R A 2004 Integrated portable genetic analysis microsystem for pathogen/infectious disease detection *Anal. Chem.* **76** 3162–70
[45] Liu Y, Foote R S, Jacobson S C, Ramsey R S and Ramsey J M 2000 Electrophoretic separation of proteins on a microchip

with noncovalent, postcolumn labeling *Anal. Chem.* **72** 4608–13
[46] Liu Y, Rauch C B, Stevens R L, Lenigk R, Yang J, Rhine D B and Grodzinski P 2002 DNA amplification and hybridization assays in integrated plastic monolithic devices *Anal. Chem.* **74** 3063–70
[47] Qiao R and Aluru N R 2002 A compact model for electroosmotic flows in microfluidic devices *J. Micromech. Microeng.* **12** 625–35
[48] Broyles B S, Jacobson S C and Ramsey J M 2003 Sample filtration, concentration, and separation integrated on microfluidic devices *Anal. Chem.* **75** 2761–7
[49] Liu R H, Yang J, Lenigk R, Bonanno J and Grodzinski P 2004 Self-contained, fully integrated biochip for sample preparation, polymerase chain reaction amplification, and DNA microarray detection *Anal. Chem.* **76** 1824–31
[50] Chan Y C, Carles M, Sucher N J, Wong M and Zohar Y 2003 Design and fabrication of an integrated microsystem for microcapillary electrophoresis *J. Micromech. Microeng.* **13** 914–21
[51] Yang R J, Fu L M and Lee G B 2002 Variable-volume-injection methods using electrokinetic focusing on microfluidic chips *J. Separation Sci.* **25** 996–1010
[52] Chang C C and Yang R J 2004 Computational analysis of electrokinetically driven flow mixing in microchannels with patterned blocks *J. Micromech. Microeng.* **14** 550–8
[53] Liao C S, Lee G B, Liu H S, Hsieh T M, Wang C H, Fan C L and Luo C H 2004 Micro reverse-transcription polymerase chain reaction system for clinical diagnosis 1998 *Proc. Micro Total Analysis Systems* pp 87–9